

Methods for determining the optimal arrangement of water deluge systems on offshore installations

Sang Jin Kim^{1,2}, Dong Hun Lee^{1,2}, Hye Min Hong^{1,2}, Se Hee Ahn^{1,2}, Jeong Beom Park^{1,2}, Jung Kwan Seo^{2*}, Bong Ju Kim², and Jeom Kee Paik^{1,2,3}

¹Department of Naval Architecture and Ocean Engineering, Pusan National University, Busan, Korea

²The Korea Ship and Offshore Research Institute (The Lloyd's Register Foundation Research Centre of Excellence), Pusan National University, Busan, Republic of Korea

³Department of Mechanical Engineering, University College London, London, Korea

Abstract

Offshore installations are prone to fire and/or explosion accidents. Fires have particularly serious consequences due to their high temperatures and heat flux, which affect humans, structures and environments alike. Due to the hydrocarbon explosions caused by delayed ignition following gas dispersion, fires can be the result of immediate ignition after gas release. Accordingly, it can be difficult to decrease their frequency, which is an element of risk (risk = frequency x consequence), using an active protection system (APS) such as gas detectors capable of shutting down the operation. Thus, it is more efficient to reduce the consequence using a passive protection system (PSS) such as water spray. It is important to decide the number and location of water deluge systems, thus the aim of this study is to introduce a new procedure for optimising the locations of water deluge systems using the water deluge location index (WLI) proposed herein. The locations of water deluge systems are thus optimised based on the results of credible fire scenarios using a three-dimensional (3D) computational fluid dynamics (CFD) tool. The effects of water spray and the effectiveness of the WLI are investigated in comparison with uniformly distributed sprays.

Keywords

offshore installations, fire accidents, optimisation of water deluge systems, water deluge location index (WLI)

1. Introduction

The operation of offshore facilities such as FPSOs, TLPs, SPARs and semi-submersibles in shallow or deep water is prone to hazardous risks. Fires and explosions account for more than 70% of accidents on offshore installations (Christou and Konstantinidou, 2012). Fires with high temperatures and heat flux result in catastrophic consequences that lead to casualties, property damage and pollution. The Piper Alpha (6 July 1998) and Deepwater Horizon (20 April 2010) accidents are typical examples of fire events (Fig. 1), and numerous fire accidents have been reported on offshore installations (Christou and Konstantinidou, 2012).

To prevent fire accidents and/or reduce their consequences, the importance of fire risk assessment and management has been magnified (Czujko and Paik, 2012a, 2012b). The risk assessment and management of fire are noted in the rules, recommended practices and design guidelines (Spouge, 1999; NORSOK, 2010; ABS, 2014; LR, 2014) and relevant guidelines have been established accordingly (Nolan, 1996; Walker et al., 2003; Vinnem, 2007; Paik and Czujko, 2009, 2010, 2011, 2012; Paik et al., 2011). The risk can be defined as

$$\text{Risk} = \text{Frequency} \times \text{Consequence} . \quad (1)$$

The two most commonly implemented risk control options are active protection systems (APSs) and passive protection systems (PPSs). APSs such as gas detectors and showdown systems are used to prevent accidents and PPSs such as water sprays, heat shields, fire and blast walls and passive fire protection (PFP) are used to address the consequences after the accidents. PPSs are usually preferred over APSs due to the latter's higher cost (Lei et al., 2015; Sohn et al., 2015), and the optimal placement of protection systems also influences their cost effectiveness.

Seo et al. (2013) introduced a methodology for optimising gas detector locations among APSs on offshore installations using a quantitative approach and a two-dimensional analytical method. Paik (2011) investigated the effects of fire walls and PFP, optimising them using quantitative fire risk assessment and management.

Although there have been numerous studies on protection systems, they have not successfully optimised the effects. Thus, the 3D CFD simulation is needed to improve the accuracy and effectiveness.

The objectives of this study are to (i) suggest a procedure to optimise water spray systems using the water deluge location index (WLI) – a new approach to selecting the optimised locations of water spray systems using the 3D CFD simulation; (ii) investigate the effects of water spray systems; and (iii) compare the proposed system with water spray systems distributed by traditional methods. Among the three types of water spray systems shown in Fig. 2, the water deluge system (Fig. 2(a)) is examined in the present study. After selecting probabilistic fire scenarios, fire CFD simulations are performed by Kameleon FireEx (KFX) CFD simulation. Then, optimised locations are suggested for water deluge systems and their performance is compared with that of uniformly distributed water sprays.

2. A procedure for the optimisation of water deluge system locations

Fig. 3 shows a procedure for the optimisation of water deluge system locations using the proposed WLI.

The procedure is composed of the following steps:

- 1) selection of credible fire scenarios;
- 2) fire CFD simulations and/or experimental tests;
- 3) obtaining the consequences of fire loads (e.g., temperature-time history, temperature distribution and temperature escalation);
- 4) definition of the operation temperatures for water deluge systems (e.g., reference temperatures);
- 5) calculation of WLI; and
- 6) selection of optimised water deluge locations.

The operation (reference) temperature can be defined by the rule, international standard, recommended practice and/or designer. For example, the National Fire Protection Association (NFPA, 1996) suggests that the operation temperature of water spray should be lower than 121°C. Designers can also suggest that the reference temperature be lower than the ‘as low as reasonably practical’ (ALARP) temperature.

3. Introducing the water deluge location index (WLI)

In this study, a ranking index – the WLI – is proposed for use in selecting optimised locations for water deluge systems. The WLI rates each space, and can be calculated as

$$WLI_i = \left[\sum_{n=1}^N \frac{(T_{R,n} - T_r)}{t_{R,n}} \right] \times \frac{F}{N}, \quad (i = 1, 2, 3, \dots, \text{total number of spaces}), \quad (2)$$

where $(T_{R,n} - T_r) / t_{R,n}$ is the slope of the temperature until the reference temperature is reached, T_R is the reference temperature, T_r is the room temperature, t_r is the time at which the reference temperature is reached, n is the scenario number, N is the total number of scenarios and F is the number of scenarios that detect a temperature above the reference temperature. If a scenario does not have a temperature above the reference temperature, the slope $((T_{R,n} - T_r) / t_{R,n})$ will be zero.

The WLI ratings can be obtained through the following steps:

- 1) definition of the reference temperature at which the water sprays operate (by rules, recommended practices, standards, etc.);
- 2) investigation of the time for each scenario at the reference temperature;
- 3) calculation of a slope of each space;
- 4) calculation of cumulative frequency for each space; and
- 5) generation of WLI in entire domain using Eq. (2).

Fig. 4 illustrates an example of spaces and temperature distribution at specific times to calculate the WLI. The size of each space (A1, A2-F5) should not exceed the capacity (i.e., radius) of the water sprays. The WLI is calculated by considering the temperature and time at each space.

Fig. 5 presents an example of nine optimised water deluge system locations obtained by the WLI in two fire scenarios.

4. Applied example of the WLI

4.1 Target structure

A hypothetical floating liquefied natural gas (FLNG) topside structure constructed by the Korea Ship and Offshore Research Institute (KOSORI) at Pusan National University was selected as the target structure to perform an applied example. It consists of three decks: the upper (solid), mezzanine (0.7 porosity) and process (solid), as shown in Fig. 6.

4.2 Selection of fire scenarios

It is important to select credible fire scenarios when making decisions about optimised water spray positions. There are numerous methods for selecting such scenarios, including standard random, stratified, Monte Carlo simulations (MCSs) and Latin hypercube samplings (LHSs) (Czujko, 2001). Among those, the LHSs use a probability density function for each variable that generates probabilistic scenarios with variable combinations. In this study, an LHS is used to select the fire scenarios because it can efficiently represent each whole scenario with a probabilistic approach. Moreover, it can cover all possible values even if they have very small probabilities.

Fig. 7 presents the scheme of the LHS technique (Ye, 1998) for selecting the fire scenarios. The LHS uses each variable value only once, and the values do not overlap, thus each variable's representative value takes the centre of the section.

Fig. 8 presents the probability density functions of the environmental and operation parameters for the LHS. Table 1 shows the 30 selected fire scenarios using the sampling technique with parameters.

4.3 Fire CFD simulations

To analyse the fire CFD simulations, the KFX (2013) CFD tool is used. Fig. 9 shows the target structure modelled in KFX and the extent of the analysis, which is a simulation volume. In this study, the modelling technique developed by Lee et al. (2014) is applied to the KFX simulations.

4.3.1 Grid convergence study

To achieve accurate and effective simulations, the grid convergence study is essential. Table 2 presents three cases with grid convergence models. All three cases have a 109x210 (mm) grid cell around the leak positions. Fig. 10 shows the results of the grid convergence study. Cases 1 and 2 show similar results, with the former having the finest grid size in the present study. Thus, the grid for case 2 is used in the CFD simulations.

4.3.2 Obtaining the fire loads in spaces for calculating the WLI

Three elevations between the decks are selected to locate the monitoring points, and the points are equally spaced to obtain the fire loads, as shown in Fig. 11. The fire loads obtained from these points are then used as the fire loads in spaces for calculating the WLI.

To calculate the WLI of each space, the districts must be divided along the spaces, as shown in Fig. 12. In this study, water sprays with a radius of 2.0 m are assumed to define the space. The average fire loads at the monitoring points in each space are applied to investigate the WLI.

4.4 Results of CFD simulations

From the simulations with 30 fire scenarios, 30 temperature distributions are obtained for each space. Fig. 13 provides examples of temperature-time histories resulting from the analysis of two spaces. Each space has different fire load characteristics, which allows the spaces to be ranked.

Fig. 14 provides examples of the temperature distributions for four fire scenarios at 2 m of elevation, 60 s after ignition. It illustrates the concept of WLI and the locations of high temperatures in each scenario.

The WLI considers a temperature at all of the time steps, although the distribution in Fig. 14 indicates specific times.

4.5 Optimisation of water deluge system locations

4.5.1 The WLI

To select optimised water deluge system locations, it is necessary to calculate the WLI developed in this study. Fig. 15 presents the temperature-time histories (shown in Fig. 13) with reference temperatures; specifically, 121°C (as suggested by the NFPA (1996)) and 500°C, for example. The averages of the slopes in all of the spaces are calculated using Eq. (2) with a reference temperature. For example, scenarios 7 and 9 have an average slope in space B3 with a 500°C reference temperature, whereas scenarios 10, 11, 12 and 26 have no score because the temperatures of scenarios 10, 11 and 12 do not reach the reference temperature. In contrast, scenarios 7, 9 and 10 have scores in space B3 with a 121°C reference temperature.

Figs. 16 and 17 show the average slopes in all of the spaces calculated using Eq. (2) with 121°C and 500°C as the reference temperatures. The slopes of 30 temperature-time histories at each space were averaged, and the scores for the average slopes were extremely different, based on the reference temperatures.

Another important factor in calculating the WLI is how frequently the temperature exceeds the reference temperature. In Fig. 18, the frequencies for the spaces are 3(B3) and 3(H3) with a 121°C reference temperature, considering only 6 scenarios in the figure. The frequencies for a 500°C reference temperature are 2(B3) and 0(H3).

Figs. 18 and 19 show the frequencies for the total number of temperatures exceeding the reference temperature (121°C or 500°C) in all of the spaces, considering 30 scenarios.

4.5.2 Proposed water deluge system locations

The WLI can be calculated using Eq. (2), which consists of the average of slopes (in Figs. 16 and 17) and frequencies (in Figs. 18 and 19). The indices can then be ranked. Table 3 shows the ranked spaces with 121°C and 500°C reference temperatures. Among them, high-ranking indices are proposed to determine the water deluge system locations.

Table 4 and Figs. 20 and 21 present the high-ranking positions and their proposed locations for 121°C and 500°C reference temperatures, assuming 9 water deluge systems. The proposed positions, based on the reference temperatures, differ from those shown in Figs. 20 and 21.

5. Efficiency of the proposed method

To verify the efficiency of the WLI in the present study, the uniformly distributed and optimised (by WLI) positions are compared. In this case, 9 water sprays are used. Fig. 22 shows the selected water deluge system locations obtained by the WLI, which is calculated with a 121°C reference temperature, as suggested by the NFPA (1996). Fig. 23 indicates the uniformly distributed water sprays.

Fig. 24 shows the comparison of the results, which are temperature distributions 40 s after ignition considered with and without water deluge systems by WLI and the uniform arrangement method. The operation time for the water sprays is 30 s after a fire.

According to the Health and Safety Executive (HSE, 2006), temperatures from 127°C to 203°C affect humans, who cannot survive exposure to temperatures above 203°C. DNV·GL (2008) investigated critical temperatures for structures, and the critical temperatures of structural and ordinary reinforcing steel are between 400-450°C.

Table 5 presents the size and number of heated areas (indices) at 40 s, which is 10 s after starting the water deluge systems with critical bounds of temperature suggested by the HSE (2006) and DNV·GL (2008). Fig. 25 illustrates the effects of water sprays on the number of heated areas, and reveals that the

WLI-optimised water deluge system locations can efficiently reduce the consequences of fire loads, compared with uniform arrangement.

Fig. 26 illustrates the time-dependent heated area below 127°C and above 700°C. It precisely shows the strength of WLI-optimised water deluge system locations.

6. Concluding remarks

The objectives of this study were to (i) suggest a new procedure for selecting efficient water deluge system locations to prevent and reduce the consequences of fire accidents on offshore installations; (ii) investigate the effects of water sprays; and (iii) compare the aforementioned results with those of the traditional method (uniformly distributed water sprays). Although the water sprays in the traditional method are uniformly located, the WLI is proposed to optimise water deluge system locations. The conclusions are as follows:

- The WLI is calculated using reference temperatures based on the operation conditions of water sprays.
- The WLI is calculated considering time-dependent temperatures.
- The WLI considers the frequency of the fire loads in each space.
- A demonstration of optimising water deluge system locations using WLI is provided with reference temperatures, and the water deluge systems are located at high-ranking indices.
- The reliability of the WLI is validated through comparison, and it is found to be more efficient than uniformly distributed systems in reducing the consequences of fire loads.

Water sprays are one method for preventing the serious damage caused by fire accidents, and for reducing the consequences of fires. The efficient placement of water deluge systems is important, as the systems are related to cost. The WLI can be helpful in optimising water deluge system locations, and it could facilitate the effective management of offshore platform risks.

Acknowledgement

This research was financially supported by the Ministry of Trade, Industry and Energy (MOTIE) and Korea Institutes for Advancement of Technology (KIAT) through the Promoting Regional Specialized (Grant no.: A010400243).

References

- ABS, 2014. Guidance noted in fire-fighting systems. American Bureau of Shipping, Texas, USA.
- Christou, M., Konstantinidou, M., 2012. Safety of offshore oil and gas operation: lessons from past accident analysis. Joint Research Centre (JRC) Scientific and Policy Reports, European Commission, Brussels, Belgium.
- Czujko, J., 2001. Design of offshore facilities to resist gas explosion hazard: engineering handbook. CorrOcean ASA, Trondheim, Norway.
- Czujko, J., Paik, J.K., 2012a. Hydrocarbon explosion and fire engineering - assessing and managing hydrocarbon explosion and fire risks in offshore installations. *Marine Technology*, pp. 23-25.
- Czujko, J., Paik, J.K., 2012b. Paradigm change in safety design against hydrocarbon explosions and fires. *FABIG Newsletter (60)*, 20-38.
- DNV·GL, 2008. DNV-OS-D301: Fire protection, Det Norske Veritas, Oslo, Norway.
- HSE, 2006. Methods of approximation and determination of human vulnerability for offshore major accident hazard assessment. Health and Safety Executive, London, UK.
- KFX, 2013. User's manual for Kameleon Fire EX. Computational Industry Technologies AS, Stavanger, Norway.
- Lee, D.H., Kim, J.H., Hong, H.M., Kim, B.J., Paik, J.K., Park, S.I., Heo, T.U., 2014. An investigation on heat reduction effect of water spray nozzle used for flare system thought comparison between the experiment and CFD simulation. In: *Proceedings of the 7th International Conference on Thin-walled Structures*, Busan, Korea.

- Lei, H.Y., Lee, J.C., Li, C.B., Ha, Y.C., Seo, J.K., Kim, B.J., Paik, J.K., 2015. Cost-benefit analysis of corrugated blast walls. *Ships and Offshore Structures* 10(5), 565-574.
- LR, 2014. Rules and regulations for the classification of offshore units - guidelines for the calculation of probabilistic explosion loads. Lloyd's Register, Southampton, UK.
- NFPA, 1996. NFPA-15: Standard for water spray fixed systems for fire protection. National Fire Protection Association, Massachusetts, USA.
- Nolan, D.P., 1996. Handbook of fire and explosion protection engineering principles for oil, gas, chemical, and related facilities. Noyes Publications, New Jersey, USA.
- NORSOK, 2010. NORSOK Standard Z-013: Risk and emergency preparedness assessment. 3rd Edition. NORSOK, Oslo, Norway.
- Paik, J.K., 2011. Report No. EFEF-04: Explosion and fire engineering of FPSOs (Phase III): nonlinear structural consequence analysis. The Korea Ship and Offshore Research Institute, Pusan National University, Busan, Korea.
- Paik, J.K., Czujko, J., 2009. Report No. EFEF-01: Explosion and fire engineering of FPSOs (Phase I): feasibility study with literature review. The Korea Ship and Offshore Research Institute, Pusan National University, Busan, Korea.
- Paik, J.K., Czujko, J., 2010. Report No. EFEF-03: Explosion and fire engineering of FPSOs (Phase II): definition of design explosion and fire loads. The Korea Ship and Offshore Research Institute, Pusan National University, Busan, Korea.
- Paik, J.K., Czujko, J., 2011. Assessment of hydrocarbon explosion and fire risks in offshore installations: recent advances and future trends. *The IES Journal Part A: Civil & Structural Engineering* 4(3), 167-179.
- Paik, J.K., Czujko, J., 2012. Engineering and design disciplines associated with hydrocarbon explosion and fire risks in offshore oil and gas facilities. *Transactions of the Society of Naval Architects and Marine Engineers* 120, 1-39.

- Paik, J.K., Czujko, J., Kim, B.J., Seo, J.K., Ryu, H.S., Ha, Y.C., Janiszewski, P., Musial, B., 2011. Quantitative assessment of hydrocarbon explosion and fire risks in offshore installations. *Mar. Struct.* 24, 73-96.
- Seo, J.K., Kim, D.C., Ha, Y.C., Kim, B.J., Paik, J.K., 2013. A methodology for determining efficient gas detector locations on offshore installations. *Ships and Offshore Structures* 8(5), 524-535.
- Sohn, J.M., Kim, S.J., Seo, J.K., Kim, B.J., Paik, J.K., 2015. Strength assessment of stiffened blast walls in offshore installations under explosions. *Ship and Offshore Structures* (Online available). <http://dx.doi.org/10.1080/17445302.2015.1035164>
- Spouge, J., 1999. A guide to quantitative risk assessment for offshore installations. DNV Technica, Oslo, Norway.
- Vinnem, J.E., 2007. Offshore risk assessment - principles, modelling and application of QRA studies. Springer, Stavanger, Norway.
- Walker, S., Bleach, R., Carney, S., Fairlie, G., Louca, L.A., 2003. New guidance on the design of offshore structures to resist the explosion hazard. In: *Proceedings of the 32nd International Conference on Ocean, Offshore and Arctic Engineering*, Cancun, Mexico.
- Ye, K.Q., 1998. Orthogonal column Latin hypercubes and their application in computer experiment. *Journal of the American Statistical Association* 93(444), 1430-1439.

Tables and Figures

Table 1 Selected fire scenarios using the LHS technique with parameters.

	Wind direction (deg.)	Wind speed (m/s)	Leak position X (m)	Leak position Y (m)	Leak position Z (m)	Leak direction	Leak rate (kg/s)
Scenario1	38.39	4.36	14.38	9.08	1.11	-Y	0.91
Scenario2	258.68	3.25	14.66	6.31	1.28	-Y	0.26
Scenario3	83.04	2.53	17.28	3.28	2.39	+Y	4.03
Scenario4	203.69	4.18	4.45	3.48	6.16	+Z	0.22
Scenario5	70.46	1.30	3.43	11.51	1.67	+Y	0.23
Scenario6	229.12	3.11	8.78	5.05	3.40	-Z	0.01
Scenario7	104.65	4.55	5.14	4.11	1.01	+Z	12.00
Scenario8	270.25	7.64	3.76	4.67	7.01	-X	0.23
Scenario9	298.41	5.55	1.82	7.50	6.16	-Z	0.82
Scenario10	195.67	5.94	3.43	9.11	1.67	-Y	9.73
Scenario11	248.14	4.01	7.40	7.60	5.24	-X	0.73
Scenario12	172.22	2.97	5.26	4.67	6.00	+X	2.05
Scenario13	164.42	6.47	5.62	3.92	6.03	+Y	0.11
Scenario14	148.60	2.68	7.26	6.26	1.47	-Y	0.57
Scenario15	211.88	3.70	5.13	8.04	5.39	+X	0.66
Scenario16	123.38	5.25	0.55	7.60	2.01	+X	0.08
Scenario17	132.07	3.55	14.10	6.52	1.28	+X	1.13
Scenario18	15.08	3.85	15.52	3.41	1.37	+Z	0.04
Scenario19	283.26	0.58	14.66	6.31	1.28	+Y	5.38
Scenario20	187.79	2.82	14.38	9.08	1.11	-Y	0.15
Scenario21	114.28	1.90	1.77	4.50	5.93	-Z	0.36
Scenario22	140.45	2.23	3.14	4.11	0.51	-X	0.74
Scenario23	179.99	1.52	2.97	8.04	5.39	-X	1.40
Scenario24	342.73	3.40	2.47	7.60	6.01	-X	0.59
Scenario25	55.96	2.39	4.45	3.48	5.94	-Z	0.46
Scenario26	94.31	4.76	4.16	6.51	5.24	+Y	3.67
Scenario27	238.34	4.99	14.10	4.52	1.28	+X	1.79
Scenario28	220.33	1.02	15.86	10.39	1.22	+Z	4.65
Scenario29	156.57	2.07	15.86	10.38	1.02	-Z	0.69
Scenario30	317.09	1.72	15.51	12.13	1.18	+Z	0.08

Table 2 Analysis cases for grid convergence study.

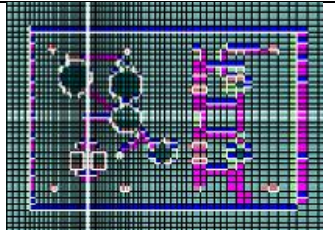
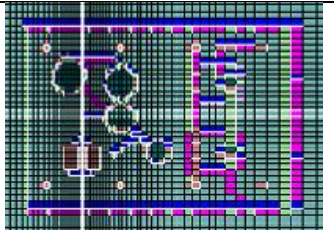
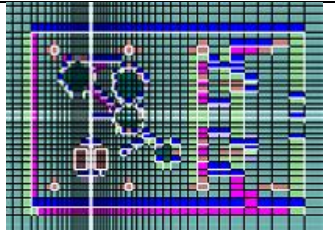
	Case 1	Case 2	Case 3
KFX view			
Number of grid cells	750,000	500,000	250,000

Table 3 Water deluge location index (WLI) ranking.

Reference Temperature = 121°C (NFPA, 1996)				Reference Temperature = 500°C			
Process - Mezzanine Deck		Mezzanine - Upper Deck		Process - Mezzanine Deck		Mezzanine - Upper Deck	
E2	11.110	I4	16.882	B4	2.974	H4	3.521
B4	10.017	J3	16.309	E2	1.974	H3	2.828
F4	8.151	J4	16.221	B3	1.267	I4	2.581
E4	7.460	I3	13.729	B5	1.117	I3	1.980
A4	6.685	I2	11.137	E1	0.825	J4	1.126
B3	5.939	H3	10.261	E4	0.716	I2	1.108
F3	5.909	H4	9.814	A4	0.520	I5	1.068
B5	4.957	I5	8.864	C4	0.506	L2	0.914
E1	4.324	J2	8.727	F4	0.428	J1	0.743
C4	3.487	L2	7.870	C5	0.270	J5	0.714
E3	3.409	I1	6.097	B2	0.224	G4	0.708
C5	3.150	J5	5.793	C3	0.222	K2	0.687
F2	2.979	J1	5.366	F2	0.212	J2	0.664
A5	2.612	K4	5.323	A3	0.212	J3	0.627
C3	2.227	L3	5.229	E5	0.197	I1	0.560
E5	2.096	K2	5.193	F1	0.156	K4	0.462
B2	2.056	K3	4.809	E3	0.137	H5	0.444
A3	2.025	H2	4.292	A5	0.121	H2	0.396
C2	1.840	G4	3.865	C2	0.116	G3	0.352
D1	1.770	H5	3.740	F3	0.111	L1	0.313
F1	1.463	G3	3.292	D5	0.023	K1	0.310
D4	1.118	K1	3.214	D4	0.023	G2	0.224
D5	0.910	L4	3.051	D2	0.004	L3	0.219
D2	0.856	K5	3.011	C1	0.003	J1	0.201
C1	0.850	L1	2.899	D1	0.003	K5	0.167
A2	0.801	G5	2.871	B1	0.001	H1	0.162
B1	0.780	H1	1.200	A1	0.000	L4	0.127
D3	0.642	G2	1.000	A5	0.000	G5	0.012
F5	0.547	L5	0.620	D3	0.000	G1	0.009
A1	0.137	G1	0.223	F5	0.000	L5	0.000

Table 4 Proposed positions for nine water deluge systems, as optimised by the WLI.

Reference Temperature = 121°C (NFPA, 1996)				Reference Temperature = 500°C			
Process - Mezzanine Deck		Mezzanine - Upper Deck		Process - Mezzanine Deck		Mezzanine - Upper Deck	
E2	11.11012	I4	16.88203	B4	2.97427	H4	3.520935
B4	10.01698	J3	16.30889	E2	1.974124	H3	2.828089
F4	8.151248	J4	16.22076	B3	1.267151	I4	2.580729
E4	7.460242	I3	13.72904	B5	1.117374	I3	1.980452
A4	6.685275	I2	11.13692	E1	0.8248	J4	1.126065
B3	5.938911	H3	10.2607	E4	0.715505	I2	1.107799
F3	5.908954	H4	9.814175	A4	0.519903	I5	1.068328
B5	4.956885	I5	8.86384	C4	0.506181	L2	0.913737
E1	4.323762	J2	8.727307	F4	0.428297	J1	0.743403

Table 5 Size of heated areas at 40 s related to critical temperatures (m²).

Temperature (°C)	*(): number of heated areas (indices)		
	Without water deluge	With water deluge (by uniform arrangement)	With water deluge (by WLI)
Below 127 (Safe)	67.2 (7)	220.8 (23)	297.6 (31)
127 - 203 (Affecting human)	57.6 (6)	124.8 (13)	76.8 (8)
203 - 400	96.0 (10)	134.4 (14)	105.6 (11)
400 - 450 (Affecting structures)	9.6 (1)	19.2 (2)	19.2 (2)
450 - 700	115.2 (12)	19.2 (2)	67.2 (7)
Above 700 (Melting point of steel)	230.4 (24)	57.6 (6)	9.6 (1)
Total	576.0 (60)	576.0 (60)	576.0 (60)



Fig. 1. Piper Alpha (6 July 1988, North Sea, left) and Deepwater Horizon (20 April 2010, Gulf of Mexico, right) accidents.



(a) Water deluge system



(b) Water mist system



(c) Water curtain system

Fig. 2. Types of water spray systems.

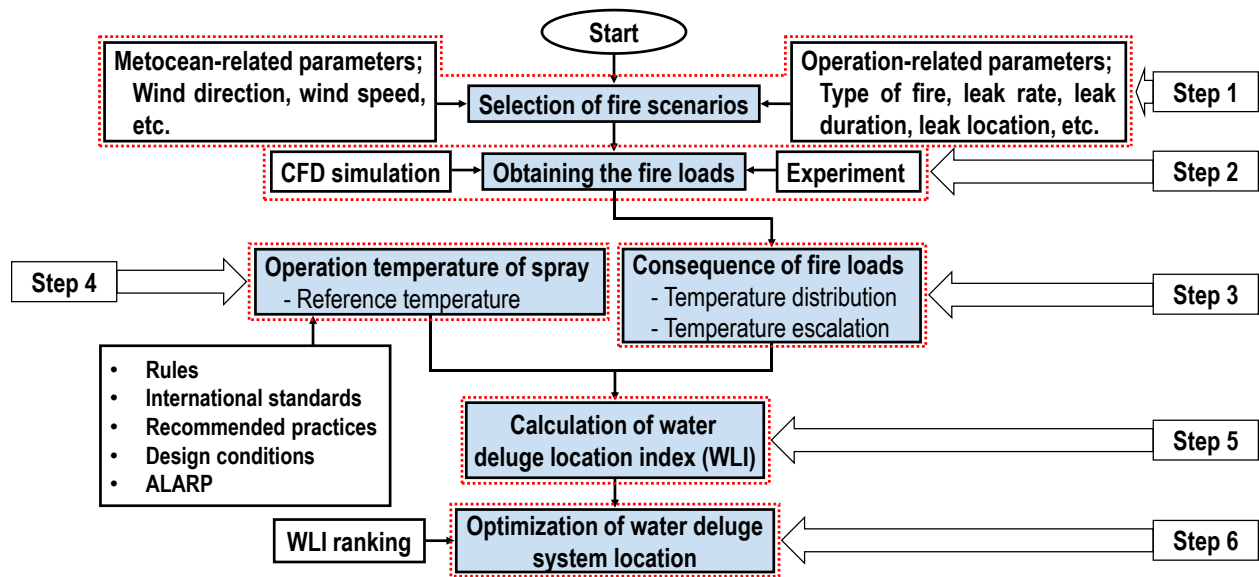


Fig. 3. Proposed procedure for the optimisation of water deluge system locations using the WLI.

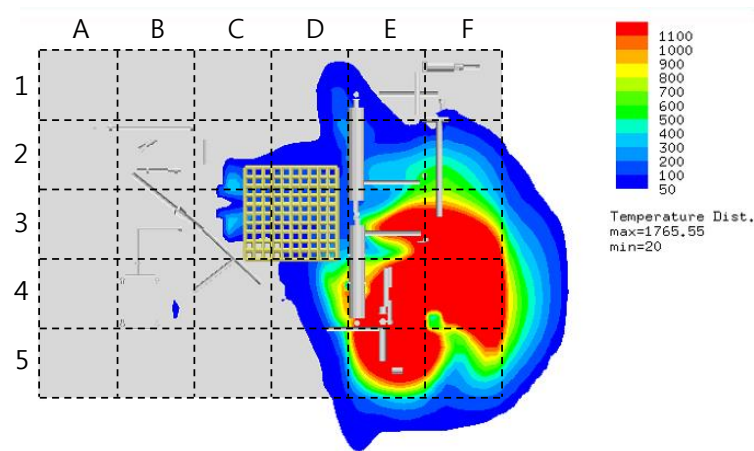


Fig. 4. An example of temperature distributions at specific times obtained by fire CFD simulation with spaces for calculating the WLI.

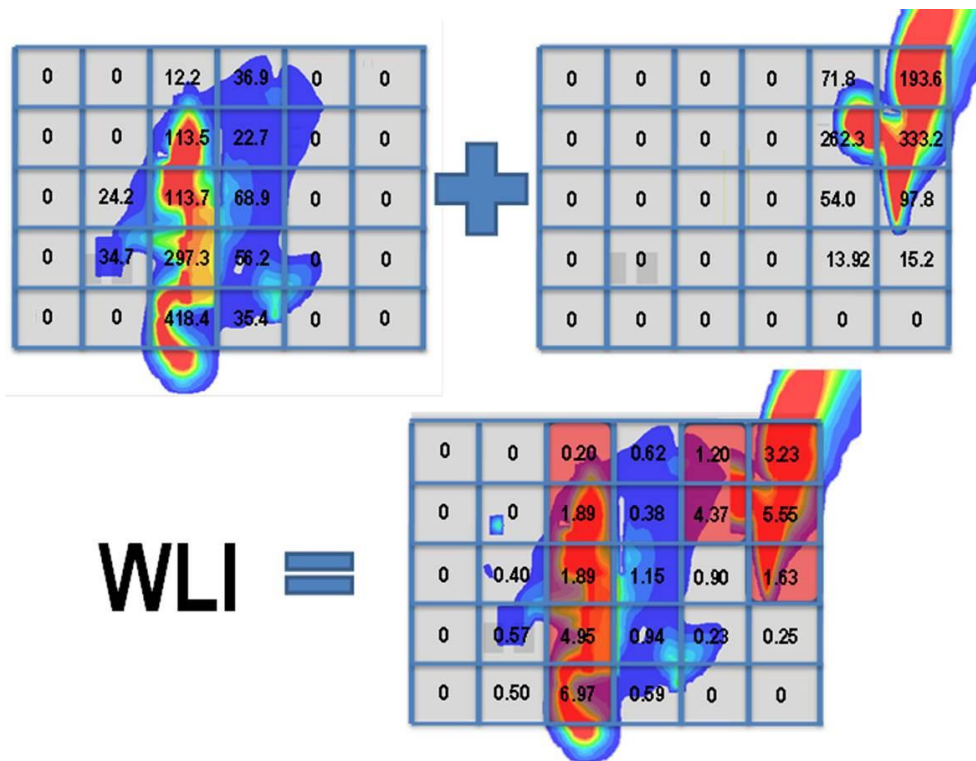


Fig. 5. An example of nine WLI-optimised water deluge system locations with two fire scenarios.

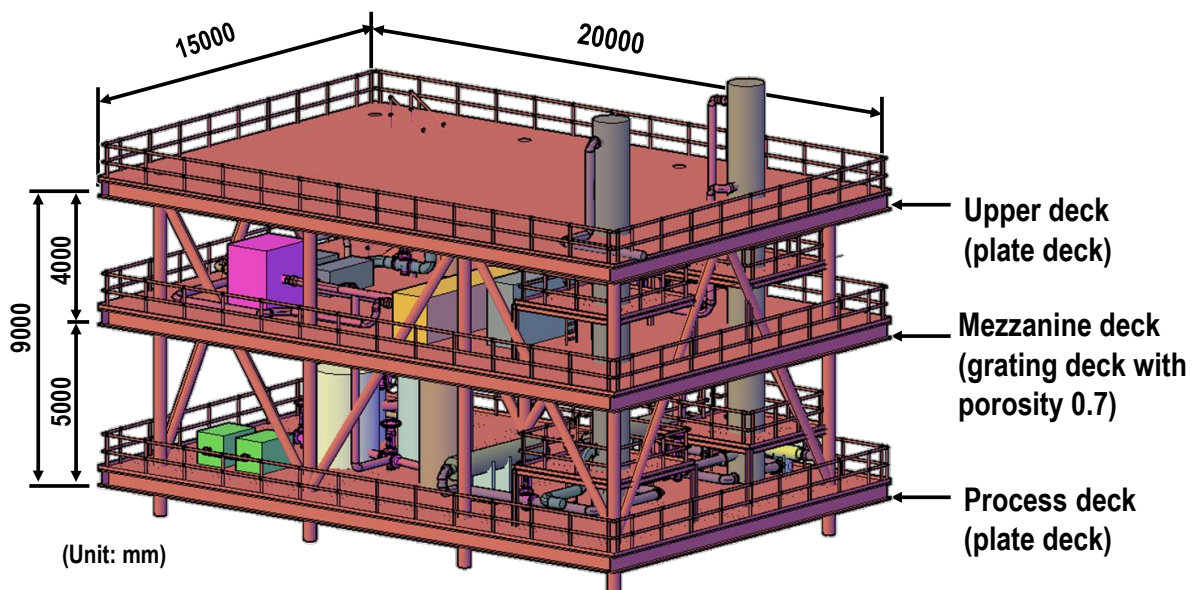


Fig. 6. The target structure (hypothetical FLNG topside module developed by KOSORI).

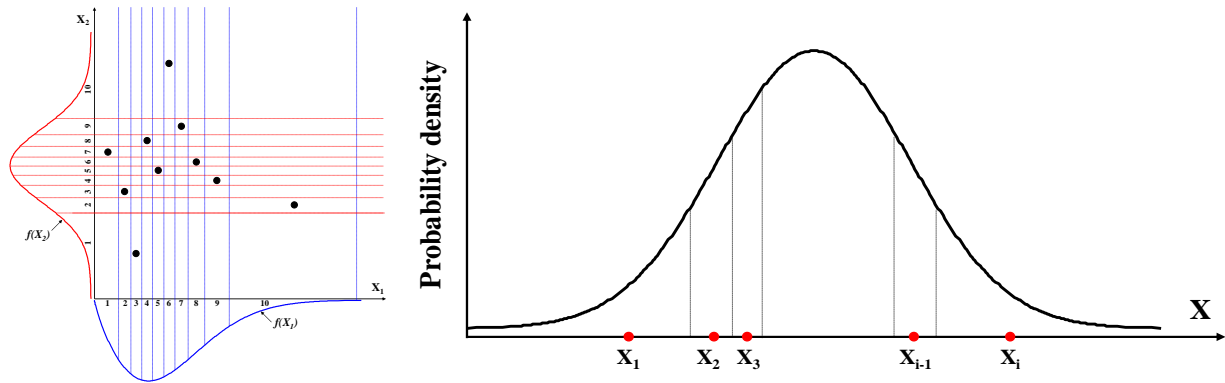
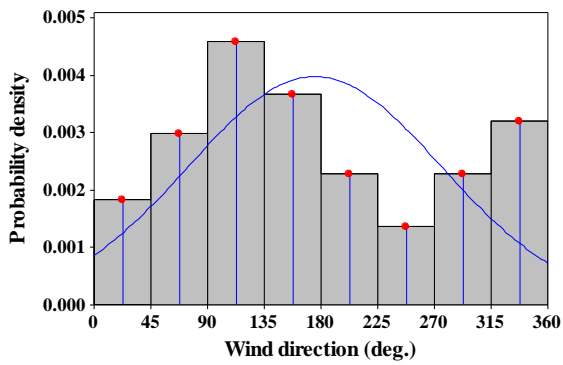
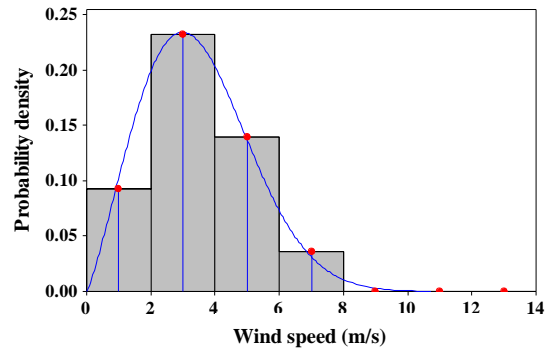


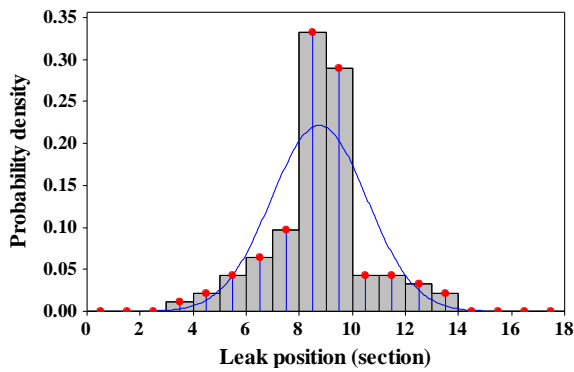
Fig. 7. Schematic of Latin hypercube sampling (LHS) technique.



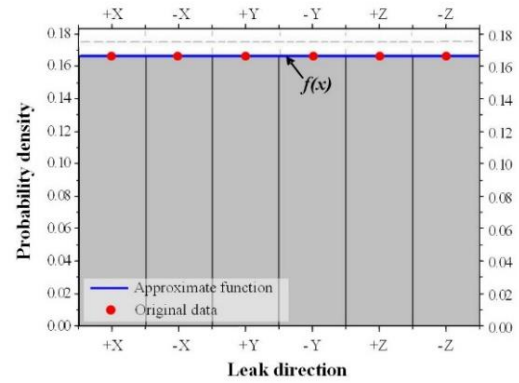
(a) Wind direction



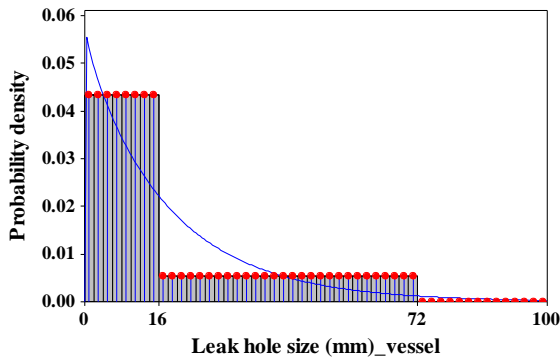
(b) Wind speed



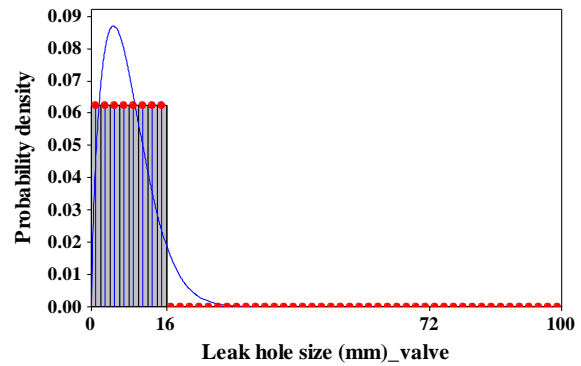
(c) Leak position



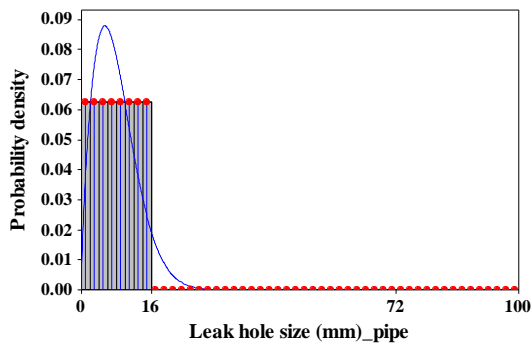
(d) Leak direction



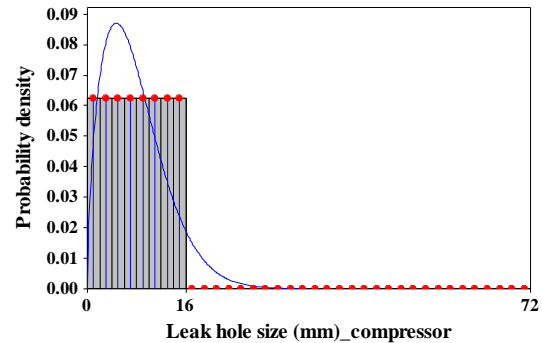
(e) Leak hole size of vessels



(f) Leak hole size of valves



(g) Leak hole size of pipes



(h) Leak hole size of compressors

Fig. 8. Probability density function of each parameter.

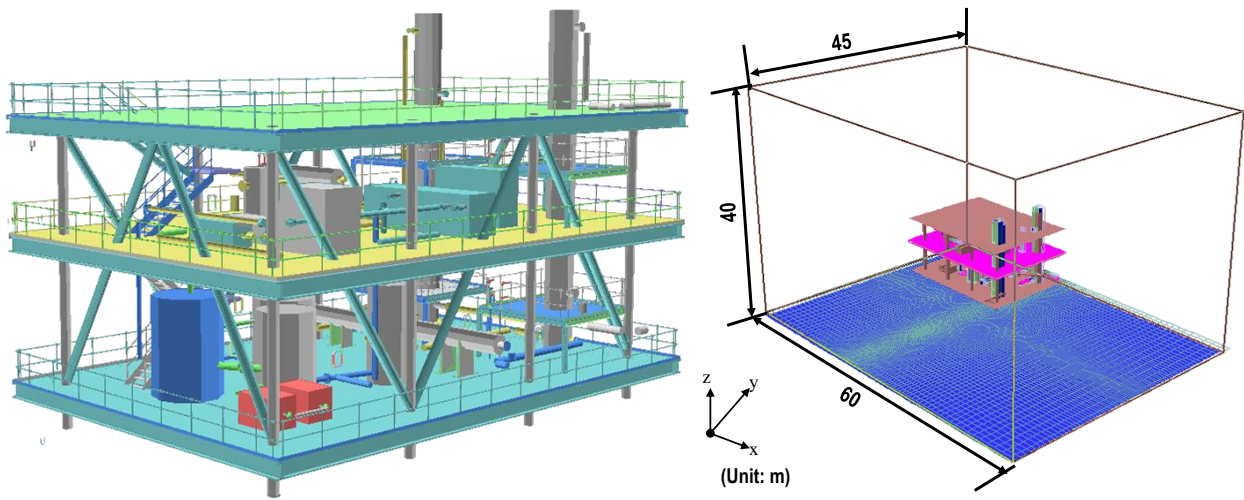


Fig. 9. Target structure modelled in KFX CFD simulation (left) and simulation volume (right).

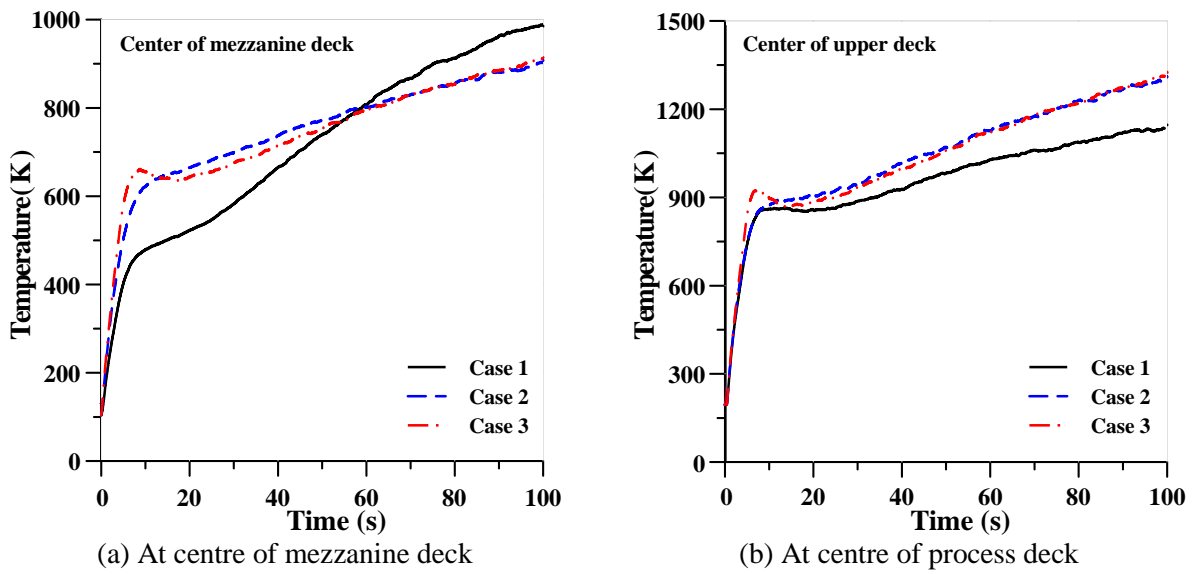
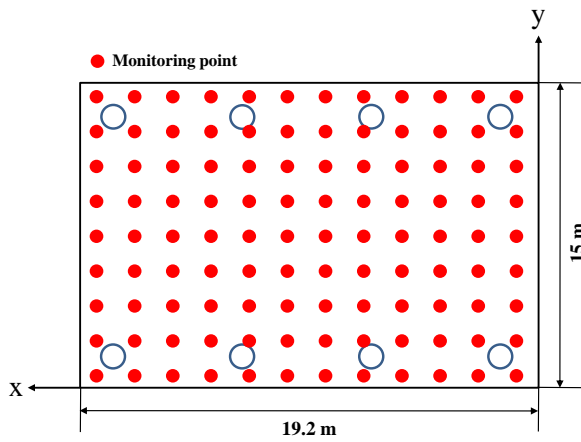
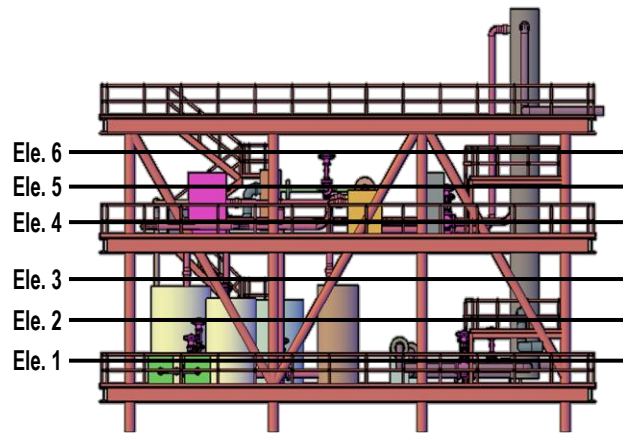


Fig. 10. Results of the grid convergence study.

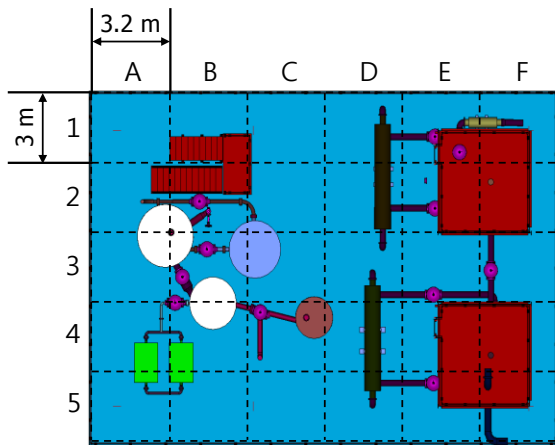


(a) Monitoring points at each elevation

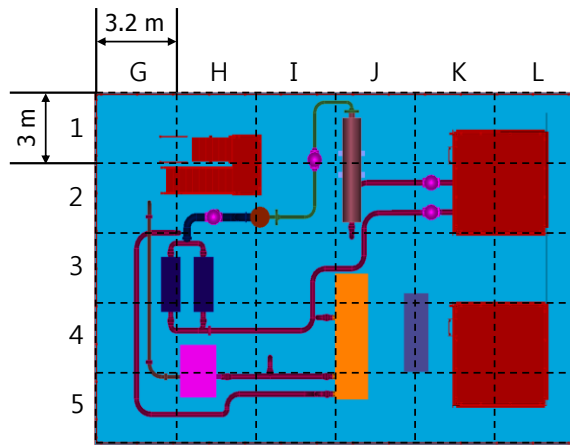


(b) Elevation levels

Fig. 11. Monitoring points to obtain the fire loads.

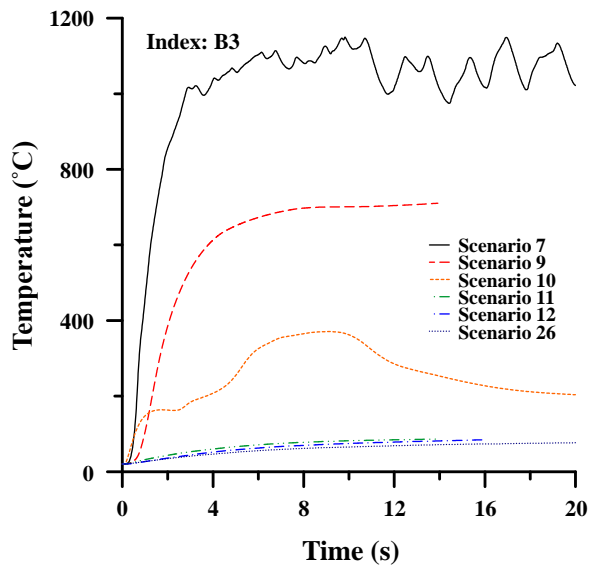


(a) Between process and mezzanine decks

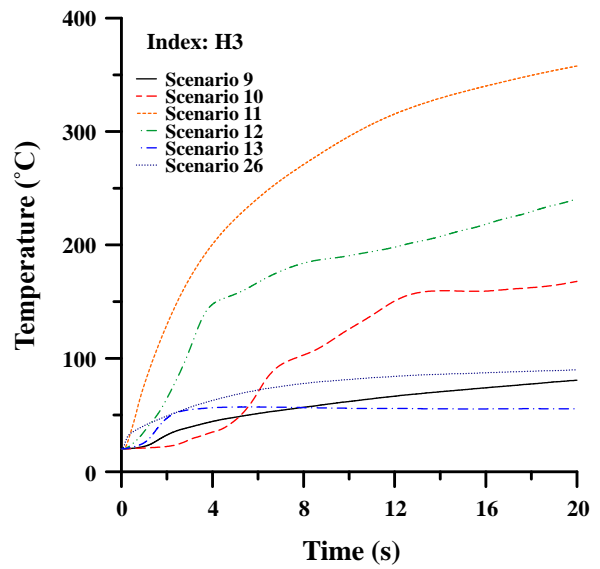


(b) Between mezzanine and upper decks

Fig. 12. Divided areas for WLI calculation.

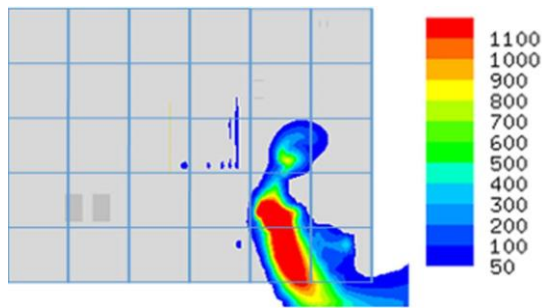


(a) Space: B3

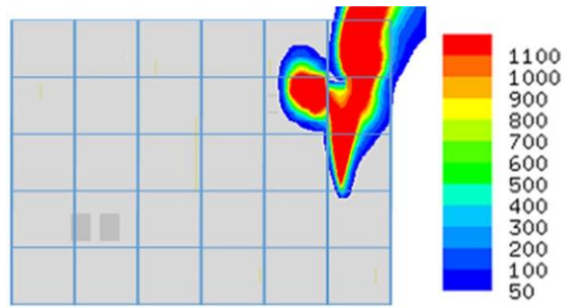


(b) Space: H3

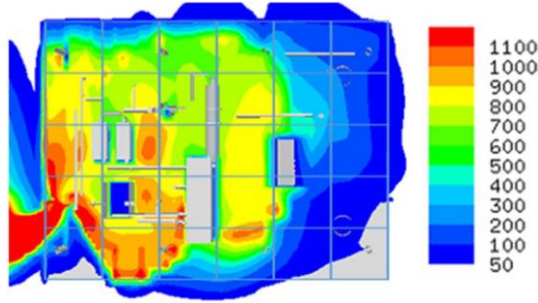
Fig. 13. Examples of the simulation results for each space.



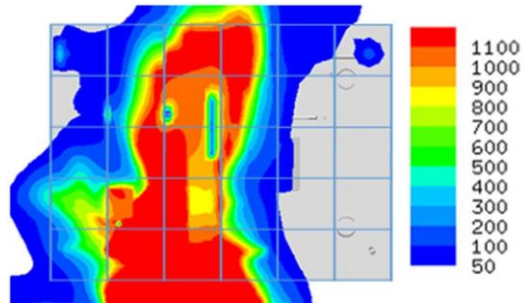
(a) Scenario 1



(b) Scenario 3

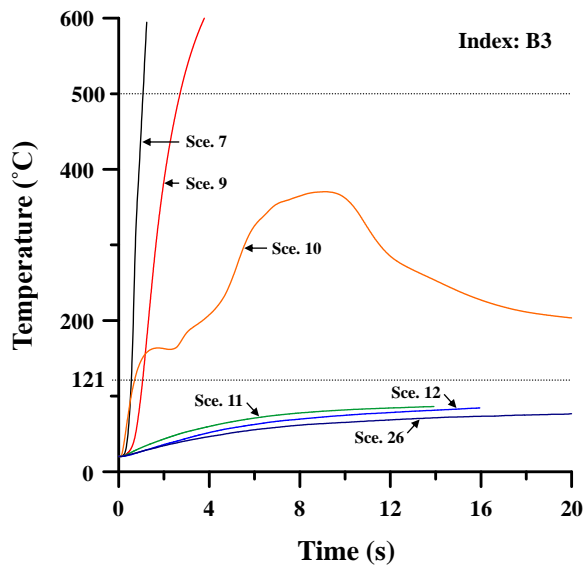


(c) Scenario 21

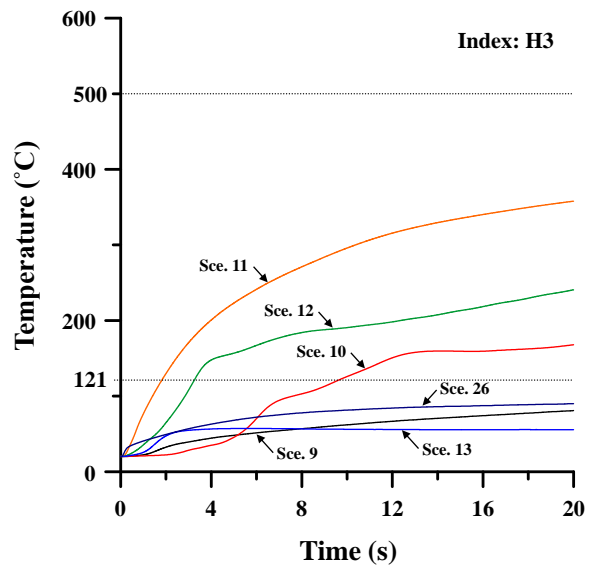


(d) Scenario 25

Fig. 14. Examples of temperature distributions at 40 s and 2 m of elevation level (°C).



(a) Space: B3



(c) Space: H3

Fig. 15. Examples of temperature-time histories for each space with reference temperatures (121°C and 500°C).

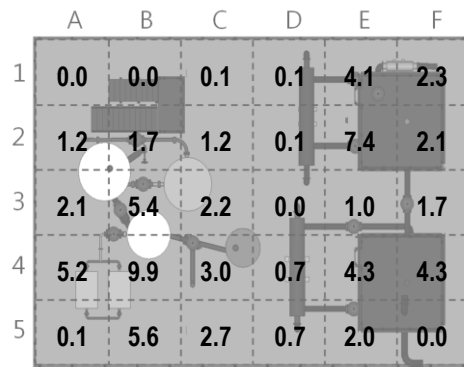
	A	B	C	D	E	F
1	1.0	2.6	2.1	3.1	10.0	5.5
2	2.7	5.1	3.1	2.0	23.8	8.9
3	5.5	13.7	5.6	1.8	7.3	10.4
4	14.3	23.1	7.5	2.6	13.2	15.3
5	7.1	13.5	7.9	3.0	5.2	2.3

(a) Between process and mezzanine decks

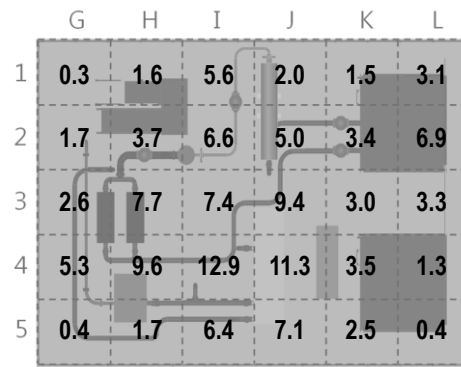
	G	H	I	J	K	L
1	1.7	3.6	13.1	8.0	6.9	7.9
2	3.7	7.6	16.7	14.5	9.7	18.2
3	7.6	19.2	21.7	25.8	10.3	8.7
4	9.7	18.4	26.7	27.0	8.4	5.4
5	7.8	8.6	17.7	15.8	6.5	2.3

(b) Between mezzanine and upper decks

Fig. 16. Average slope of the temperature-time history up to the reference temperature for each space, considering all scenarios (reference temperature = 121°C).

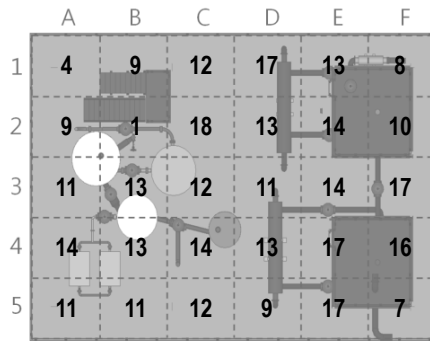


(a) Between process and mezzanine decks

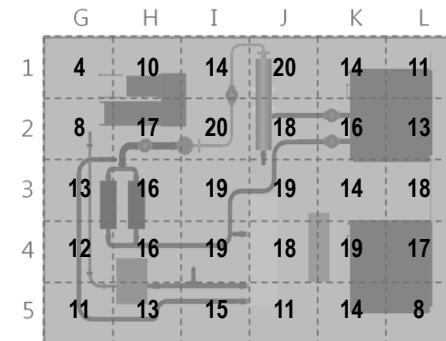


(b) Between mezzanine and upper decks

Fig. 17. Average slope of the temperature-time history up to the reference temperature for each space, considering all scenarios (reference temperature = 500°C).

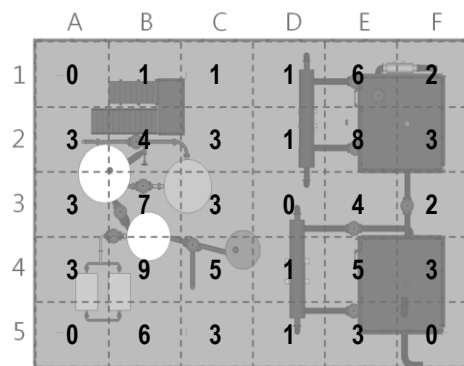


(a) Between process and mezzanine decks

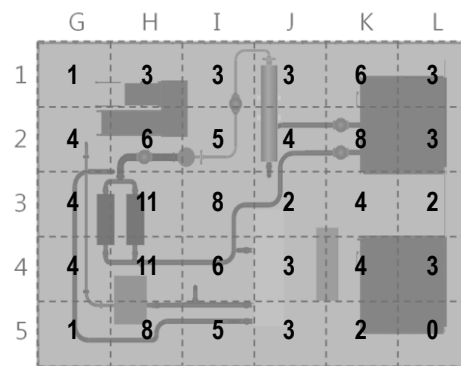


(b) Between mezzanine and upper decks

Fig. 18. Frequencies (F) that detect the reference temperature for each space, considering all scenarios (reference temperature = 121°C).

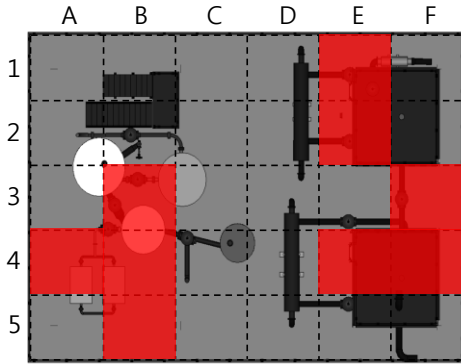


(a) Between process and mezzanine decks

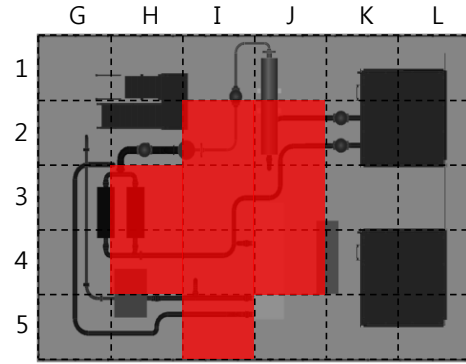


(b) Between mezzanine and upper decks

Fig. 19. Frequencies (F) that detect the reference temperature for each space, considering all scenarios (reference temperature = 500°C).

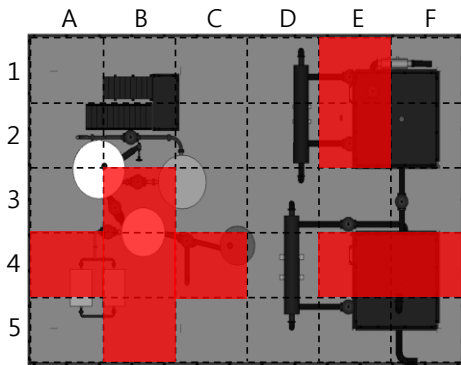


(a) Between process and mezzanine decks

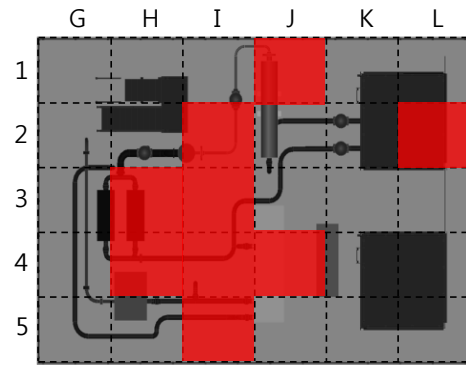


(b) Between mezzanine and upper decks

Fig. 20. Nine high-ranking locations by WLI (reference temperature = 121°C).

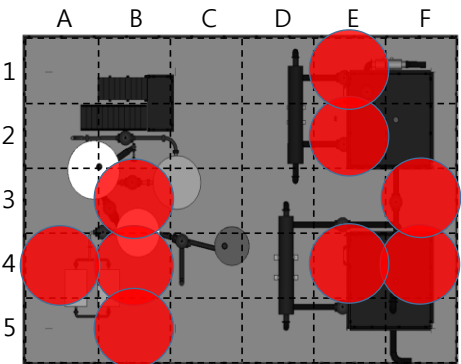


(a) Between process and mezzanine decks

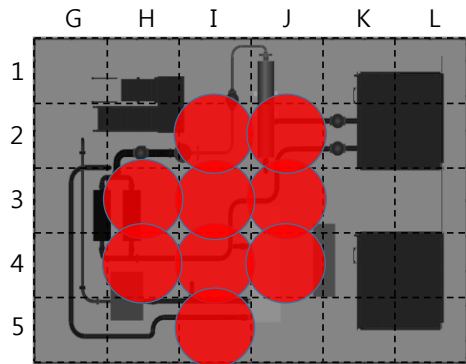


(b) Between mezzanine and upper decks

Fig. 21. Nine high-ranking locations according to the WLI (reference temperature = 500°C).

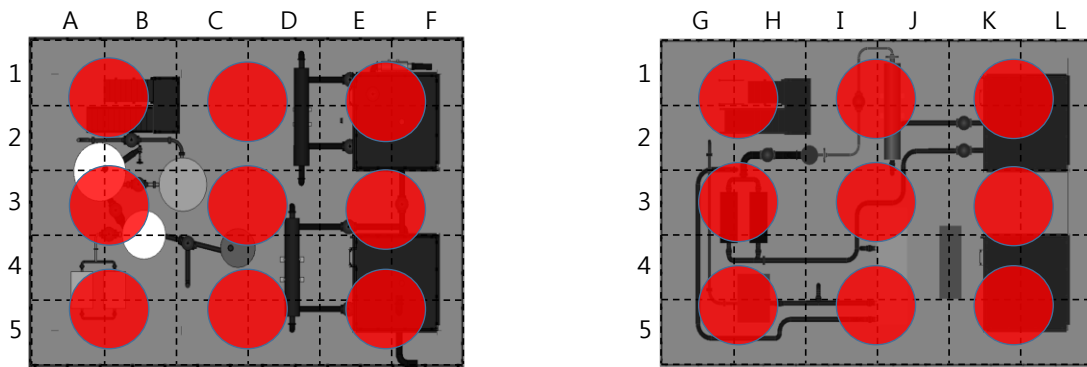


(a) Between process and mezzanine decks



(b) Between mezzanine and upper decks

Fig. 22. WLI-optimised water deluge system locations.



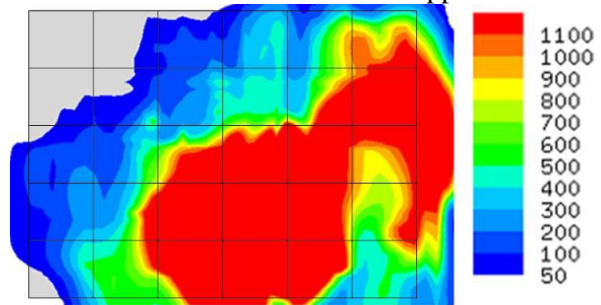
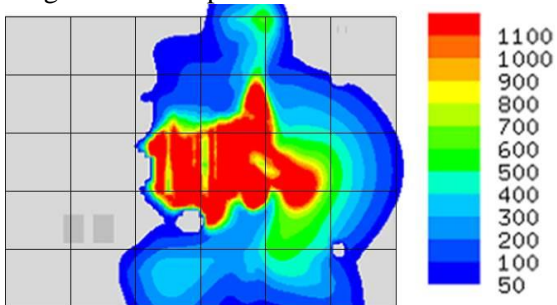
(a) Between process and mezzanine decks

(b) Between mezzanine and upper decks

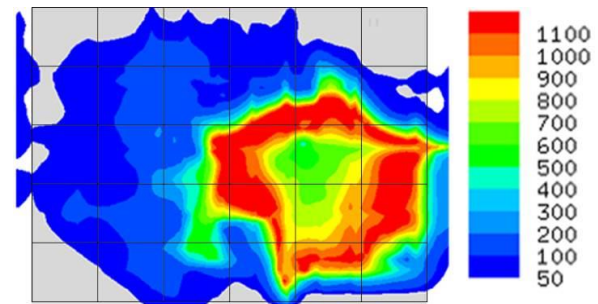
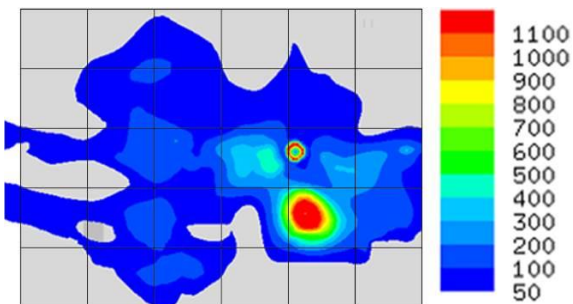
Fig. 23. Water deluge system locations according to the uniform arrangement method.

Right: Between process and mezzanine decks

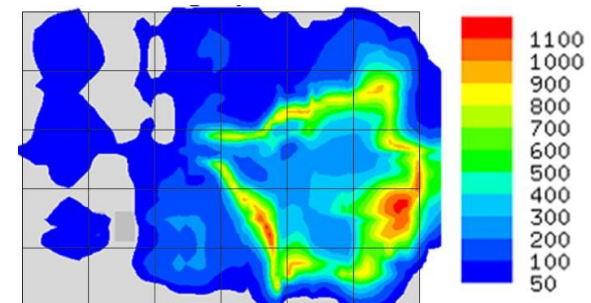
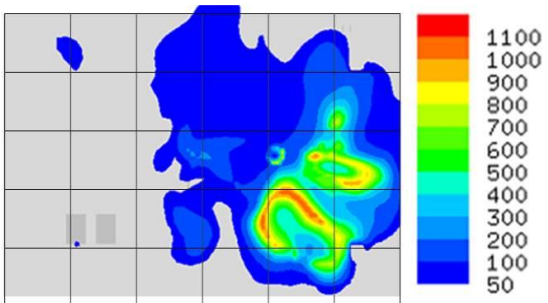
Left: Between mezzanine and upper decks



(a) Without water deluge system



(b) With uniformly distributed water deluge systems



(c) With WLI-optimised water deluge systems

Fig. 24. Comparison of temperature distributions 60 s after ignition, without and with water deluge systems ($^{\circ}\text{C}$).

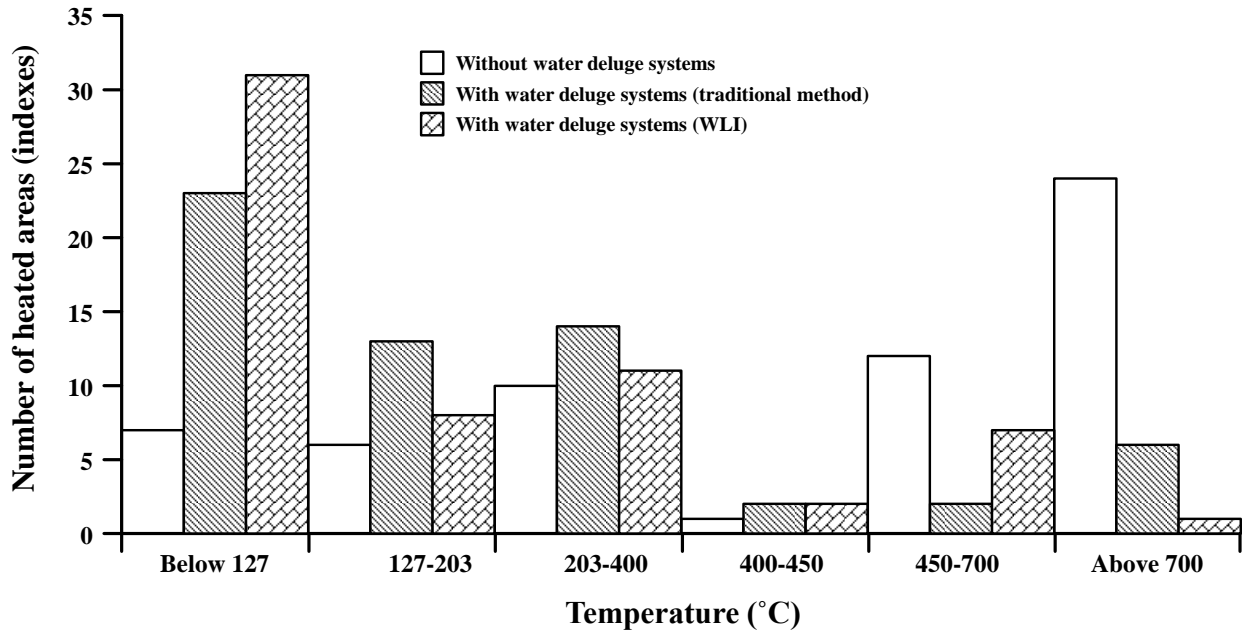


Fig. 25. Effects of water sprays on the number of heated areas.

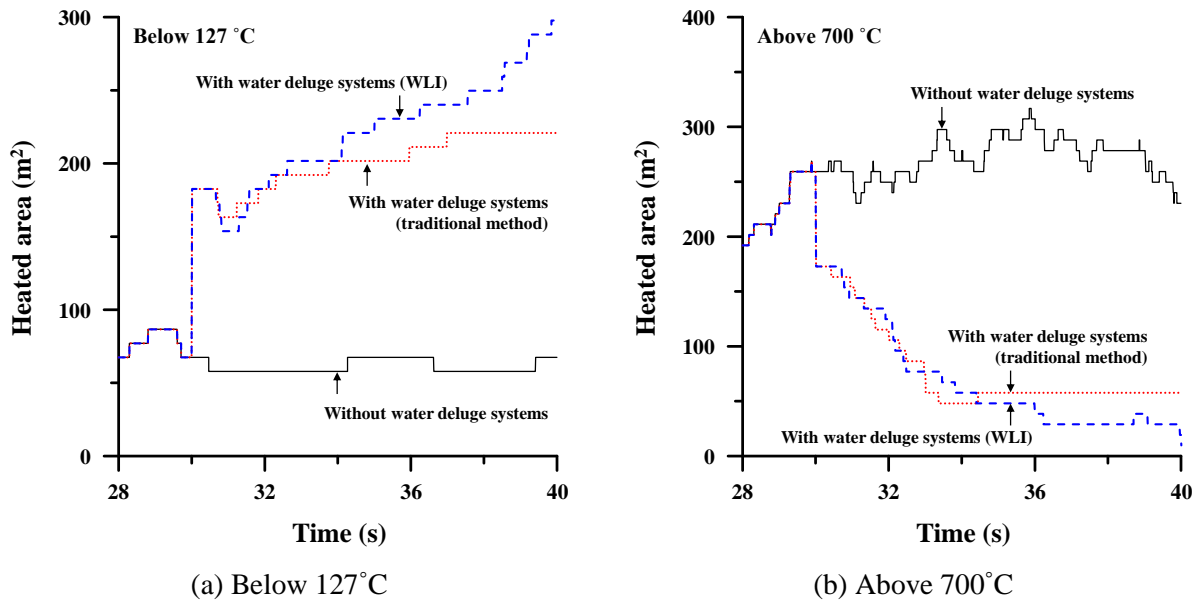


Fig. 26. Comparison of time dependent heated area, without and with water deluge systems.